UCLouvain
Institute of Mechanics,
Materials and Civil Engineering

Numerical methods for granular media in multiphase fluids

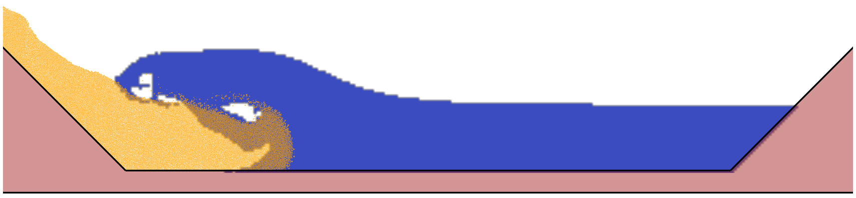

Michel HENRY

Thesis typescript submitted in partial fulfilment of the requirements
for the Ph.D Degree in Engineering Science

Thesis Committee

Advisors	Vincent LEGAT Jonathan LAMBRECHTS	UCLouvain UCLouvain
Jury	Frédéric DUBOIS Nicolas MOËS Miguel CABRERA Olivier BRULS Stéphane DORBOLO	CNRS-LMGC/UM UCLouvain TUDelft ULiège ULiège
Chairperson	Paul FISETTE	UCLouvain

Louvain-la-Neuve, 9th September 2025

CHAPTER 2

Non-Smooth Dynamics in Granular Physics

If you can't explain it simply, you don't understand it well enough.

— Albert Einstein.

Granular materials consist of macroscopic particles that interact through contact forces, friction, and collisions. Unlike fluids or conventional solids, granular matter lacks a clear scale separation between microscopic interactions and macroscopic behaviour, making it difficult to describe with classical continuum mechanics [65, 66, 67]. In particular, defining consistent constitutive laws, that relate stress and strain in a predictive way, is challenging due to the discrete nature of the medium, history dependence, and strong heterogeneities in force transmission [68]. These limitations motivate the use of numerical approaches that resolve grain-scale interactions directly.

One such approach is the Discrete Element Method (DEM) originally developed by Cundall and Strack [36] for geomechanical problems. Particles are modeled as rigid bodies whose motion and contact interactions are governed by Newton-Euler's laws of motion. By treating grains as rigid bodies, DEM avoids the need to define bulk constitutive relationships, instead computing macroscopic responses as an emergent result of contact-level physics. Each grain's position and orientation evolve according to forces arising from inter-particle contacts, gravity, and possibly fluid interactions. This particle-scale resolution provides a natural way to capture phenomena such as jamming, segregation, dilatancy, and energy dissipation. These features are difficult to encode in continuum models [69, 70, 71].

Traditional implementations of the Discrete Element Method (DEM) often rely on smooth contact laws, whereby small overlaps between particles are used to model elastic or viscoelastic behaviour [72]. This approach, known as the soft-sphere model, enables efficient explicit time integration, which is particularly well-suited for GPU-based parallelization [37]. While effective for loosely packed or weakly interacting granular systems, soft-sphere DEM can encounter stability and efficiency issues when applied to densely packed, stiff, or quasi-rigid materials. In these regimes, large numbers of simultaneous contacts and rapidly changing contact networks can lead to numerical instabilities and require prohibitively small time steps to maintain accuracy and robustness. To overcome these limitations, the Non-Smooth Contact Dynamics (NSCD) approach has been developed [73, 74, 75]. NSCD treats particles as perfectly rigid bodies and resolves contact interactions through complementarity conditions or variational inequalities, which enforce non-penetration and Coulomb friction constraints directly, without relying on artificial dissipation or elastic deformation. This framework is particularly advantageous for modelling dense granular flows, where persistent contacts, sudden transitions between sticking and sliding, and highly intermittent force chains are common. Unlike soft-sphere, NSCD is capable of resolving large contact networks and discontinuous motion in a stable and consistent manner, without requiring small time steps or the regularization of contact laws. This makes it especially suitable for applications such as quasi-static deformation, compaction, or impact-driven granular dynamics, where the accurate treatment of contact conditions is critical.

In real-world scenarios, granular flows often occur in the presence of an interstitial fluid, such as air or water. The interaction between the grains and the fluid can dramatically influence the flow behaviour due to added mass effects, buoyancy, drag, lubrication, and variations in pore pressure. The force applied by the fluid to each grain can be incorporated directly into the DEM framework through an external fluid-grain interaction force. This external force can be explicitly integrated into the NSCD framework, enabling the simulation of immersed granular flows. Additionally, since overlapping particles are not allowed, the numerical scheme naturally satisfies particle volume conservation.

The Discrete Element Method (DEM) can be summarised as follows. Algorithm 1 provides an overview of the key steps involved in a single time step of the DEM. First, the *free velocity* of each particle is computed by integrating the external forces (such as gravity and fluid–grain interactions) over the time step, assuming no contact interactions. Next, the *contact detection* step identifies all potential contacts between particles and between particles and boundaries. These contacts are used to formulate the contact constraints, such as non-penetration and frictional sliding. Once contacts have been detected, the *contact problem* is solved using a Non-Smooth Contact Dynamics (NSCD) approach. This involves computing the *contact impulse* necessary to enforce the contact constraints. This impulse is then applied to adjust the velocities so that they satisfy both Newton's laws and the contact conditions. Finally, the particle positions and orientations are updated using the post-contact velocities, thus completing the time step. These updated states are then used to advance to the next time step in the simulation.

In this chapter, we present the fundamentals of the Discrete Element Method as applied to the particulate phase in fluid–granular systems, with a focus on its non-smooth dynamics formulation. We detail the theoretical framework of NSCD and its numerical implementation.

Algorithm 1: Iteration of a DEM Solver.

Require: $\mathbf{q}^n, \mathbf{v}^n, \mathbf{f}_e^n, \Delta t$

$\mathbf{v}^- \leftarrow \mathbf{v}^n + \Delta t \mathbf{f}_e^n$

$\mathcal{C} \leftarrow$ Contact Detection

$\mathbf{p}^{n+1}, \mathbf{v}^{n+1} \leftarrow$ Solve the contacts problem

$\mathbf{q}^{n+1} \leftarrow$ Update the bodies position

Contents

2.1 Non-Smooth Newton–Euler Dynamics

Originally developed for geomechanical applications [36], the Discrete Element Method (DEM) has evolved into a widely adopted numerical approach for simulating the behaviour of granular materials. In this framework, each particle is modelled as a rigid body, and its motion is governed by the Newton–Euler equations. The discontinuous nature of collisions and contact interactions necessitates a non-smooth formulation of the dynamics. Generalised configuration variables are introduced to describe the particle's position and orientation, providing a comprehensive representation of its motion. This formulation leads to a concise set of equations that govern the particle's dynamics, including both linear and angular momentum balances which will be suitable to describe the contact dynamics.

2.1.1 Rigid body kinematics

A rigid body can be described using generalised coordinates, which represent its position $\mathbf{y} \in \mathbb{R}^3$ and its orientation, represented by a unit quaternion $\boldsymbol{\theta} \in \mathbb{H}^4$ in the Euclidean space $\mathbb{R}^3$. For two-dimensional systems, a single angle is sufficient to describe the orientation. For numerical purposes, unit quaternions are often preferred to Euler angles or a rotation matrix due to their computational efficiency and numerical stability. The generalised velocity, denoted $\mathbf{v}$, relates the generalised coordinates to the linear and angular velocities in the body-fixed reference frame:

$$\mathbf{q} = \begin{bmatrix} \mathbf{y} \\ \boldsymbol{\theta} \end{bmatrix}, \qquad \mathbf{v} = \begin{bmatrix} \dot{\mathbf{y}} \\ \boldsymbol{\omega} \end{bmatrix} \tag{2.1}$$

where $\dot{\mathbf{y}} \in \mathcal{R}^3$ is the linear velocity and $\boldsymbol{\omega} \in \mathcal{R}^3$ is the angular velocity.

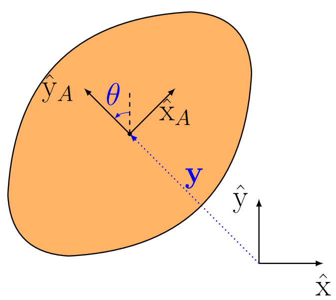

Figure 2.1: Configuration variables of a rigid body.

The time derivative of the orientation, $\boldsymbol{\theta} \in \mathbb{H}^4$ is related to the angular velocity, $\boldsymbol{\omega} \in \mathbb{R}^3$ by:

$$\dot{\boldsymbol{\theta}} = \frac{1}{2}\mathbf{Q}(\boldsymbol{\theta})\boldsymbol{\omega} \tag{2.2}$$

$$\dot{\boldsymbol{\theta}} = \frac{1}{2}\begin{bmatrix} -\omega_x\theta_x - \omega_y\theta_y - \omega_z\theta_z \\ \omega_x\theta_w + \omega_y\theta_z - \omega_z\theta_y \\ \omega_y\theta_w - \omega_x\theta_z + \omega_z\theta_x \\ \omega_z\theta_w + \omega_x\theta_y - \omega_y\theta_x \end{bmatrix} \tag{2.3}$$

It follows that the time derivative of the generalised coordinates $\mathbf{q}$ can be expressed as:

$$\dot{\mathbf{q}} = \mathbf{T}(\mathbf{q})\mathbf{v} \tag{2.4}$$

where $\mathbf{T}(\mathbf{q})$ is the transformation matrix from the generalised velocities to the generalised coordinates based on Equation (2.3). The generalised coordinates are defined by six degrees of freedom in three-dimensional space and three degrees of freedom in two-dimensional space. Figure 2.1 illustrates the rigid body configuration.

2.1.2 Non-Smooth Dynamics

The dynamics of a rigid body are governed by the Newton–Euler equations, which describe the motion of the particle in terms of its linear and angular momentum. External impulses act on the particle, which can be due to contact forces, fluid forces, or external forces such as gravity. Figure 2.2 illustrates the motion of a particle subjected to gravity and an external forces. To account for the non-smooth nature of contact interactions, the dynamics equations are formulated in a differential form [76, 74] :

$$\mathbf{M}\mathrm{d}\mathbf{v} = \mathbf{f}_\mathrm{e}\mathrm{d}t + \mathbf{f}_\mathrm{q}\mathrm{d}t + \mathrm{d}\mathbf{p} \tag{2.5}$$

where $\mathrm{d}\mathbf{v}$ is the differential measure of the velocity, $\mathbf{f}_\mathrm{e}$ is the external generalised force, $\mathrm{d}\mathbf{p}$ is the generalised impulse and $\mathbf{M}$ is the generalised mass matrix defined as:

$$\mathbf{M} = \begin{bmatrix} m\mathbf{I} & \mathbf{0} \\ \mathbf{0} & \mathbf{J} \end{bmatrix} \tag{2.6}$$

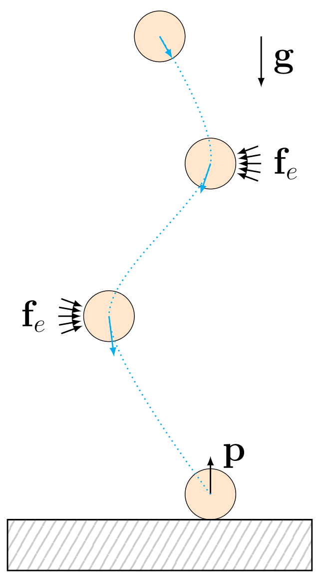

Figure 2.2: A disc subjected to external forces.

where m is the mass of the body, $\mathbf{I} \in \mathbb{R}^{3\times3}$ is the identity matrix, $\mathbf{J} \in \mathbb{R}^{3\times3}$ is the inertia matrix and $\mathbf{0} \in \mathbb{R}^{3\times3}$ is the null matrix. The generalised external force $\mathbf{f}_\mathrm{e}$ includes the external forces and moments acting on the particle, such as gravity or fluid forces. Contact forces and moments are included in the generalised impulse. Gyroscopic moments are included in the generalised quadratic force $\mathbf{f}_\mathrm{q}$, which is defined as:

$$\mathbf{f}_\mathrm{q} = \begin{bmatrix} \mathbf{0} \\ -\boldsymbol{\omega} \times \mathbf{J}\boldsymbol{\omega} \end{bmatrix} \tag{2.7}$$

For a sphere or bidimensional system, the quadratic force is zero because the inertia matrix is diagonal. This term will be omitted from the following equations, since only two-dimensional systems and symmetric particles will be considered. To model contact interactions, inequalities are used to enforce non-penetration and frictional constraints. The Discrete Element Method (DEM) solves the equations of motion for each particle in the system, Equation (2.5), neighboring particles interact through contact forces and moments.

In order to address the discontinuous nature of the contact impulse, the generalised velocity $\mathbf{v}$ is assumed to be a right continuous locally bounded variation function. This means that the measure of $]t_0, t]$ by $\mathrm{d}\mathbf{v}$ is

$$\int_{]t_0,t]} \mathrm{d}\mathbf{v} = \mathbf{v}(t) - \mathbf{v}(t_0). \tag{2.8}$$

The kinematics and dynamics of a rigid body in the non-smooth framework can be expressed as:

$$\mathbf{q}(t) - \mathbf{q}(t_0) = \int_{]t_0,t]} \mathbf{T}(\mathbf{q})\ \mathrm{d}\mathbf{v}, \tag{2.9}$$

$$\mathbf{M}\Big(\mathbf{v}(t) - \mathbf{v}(t_0)\Big) = \int_{]t_0,t]} \mathbf{f}_\mathrm{e}\ \mathrm{d}t + \mathbf{p}. \tag{2.10}$$

The unknowns in these equations are the generalised coordinates $\mathbf{q}$, the generalised velocities $\mathbf{v}$, and the generalised impulses $\mathbf{p}$. In practice, the external force $\mathbf{f}_\mathrm{e}$ is integrated explicitly, and the *free velocity* $\mathbf{v}^-$ is defined as the velocity the body would get in the absence of contact interactions:

$$\mathbf{v}^- = \mathbf{v}(t_0) + \mathbf{M}^{-1}\mathbf{f}_\mathrm{e}\Delta t, \tag{2.11}$$

where $\mathbf{M}$ is the mass matrix and Δt is the time step. It leads to the following expression for the body dynamics:

$$\mathbf{M}(\mathbf{v}^+ - \mathbf{v}^-) = \mathbf{p}, \tag{2.12}$$

where $\mathbf{v}^+$ and $\mathbf{v}^-$ denote the post and pre-impact velocities, respectively. The unknown quantities in this equation are the post-impact velocity $\mathbf{v}^+$ and the contact impulse $\mathbf{p}$. The next section introduces the *Contact Dynamics* method, which uses non-overlapping and frictional contact constraints to determine these quantities.

2.2 Contact Dynamics

The core principle of the Non-Smooth Contact Dynamics (NSCD) method is to treat contact events as discontinuous impulse. All contacts occurring within a time step are considered instantaneous and are solved simultaneously. This approach enables the simulation of contact dynamics even when the duration of contact tends toward zero. However, a fundamental trade-off of this method is the loss of uniqueness of the solution, meaning that multiple valid outcomes may exist for a given configuration. The method can be divided into three main stages:

Contact Detection involves identifying potential contact pairs. This is done by computing the distance between particles and checking whether they are sufficiently close to interact. A naive approach would involve checking all possible particle pairs, but this becomes computationally infeasible for large systems. To address this issue, tree-based spatial partitioning algorithms are employed to efficiently detect potential contacts using particle bounding boxes. As a consequence of the detection step, a time step restriction arises from this stage to ensure accurate detection.

Local Contact Resolution Once potential contacts have been identified, each one is treated individually. A local contact frame is then defined at each contact point to serve as the reference basis for expressing contact conditions. Within this frame, non-overlapping constraints, friction, and inelastic collision conditions are formulated as inequalities. The contact dynamics are therefore expressed in terms of complementarity conditions within this local frame.

Global Resolution Solving the full contact problem involving multiple interacting bodies requires iterative algorithms. Since multiple contacts can act simultaneously on a single body, the contact problem is inherently coupled and nonlinear. To handle these interdependencies and ensure a consistent global solution, iterative schemes are employed to progressively converge towards a stable configuration. Commonly used methods include the *Nonlinear Gauss–Seidel* algorithm [40, 77], *Conjugate Gradient* *methods* [78], and optimisation-based approaches such as the *Accelerated Gradient Scheme* [39].

This section details the procedures for both local and global contact resolution. First, we introduce the kinematics of contact, including the definition of the contact frame and the associated transformation matrix. Next, we present Signorini's condition, which enforces the non-penetration constraint between interacting bodies. This is followed by a discussion of Coulomb's friction law, which governs the tangential forces that arise at contact points. Finally, we describe the Gauss–Seidel algorithm, an efficient iterative method for solving the global multi-contact problem.

2.2.1 Contact Kinematics

To express the equations of motion in the local frame, we introduce a local frame associated with the contact point. Let $\mathbf{n}$ be the unit normal vector to the contact plane and $\mathbf{s}$ and $\mathbf{t}$ be the two tangential vectors in the contact plane. The normal vector is defined as the unit vector pointing from the two closest point between body A and body B. It leads that the gap between the two bodies is given by,

$$g(t) = \mathbf{n} \cdot (\mathbf{y}^{\mathrm{c}}_A - \mathbf{y}^{\mathrm{c}}_B), \tag{2.13}$$

where $\mathbf{y}^{\mathrm{c}}_A$ is the closest point from body A to body B and $\mathbf{y}^{\mathrm{c}}_B$ is the closest point to body A on body B. Figure 2.3 illustrates the local frame associated with the contact point.

We seek to express the equations of motion in the local frame associated with the contact point. The absolute velocity at the contact point in the global frame is given by :

$$\begin{aligned} \mathbf{v} &= \dot{\mathbf{y}} + \boldsymbol{\omega} \times \mathbf{y}^{\mathrm{c}}, && (2.14) \\ &= \begin{bmatrix} \mathbf{I} & \mathbf{R} \end{bmatrix} \begin{bmatrix} \dot{\mathbf{y}} \\ \boldsymbol{\omega} \end{bmatrix} && (2.15) \\ & && (2.16) \end{aligned}$$

where $\mathbf{I}$ is the identity matrix, $\mathbf{R}$ the skew-symmetric matrix use to express the vector cross-product as a matrix-vector product:

$$\mathbf{R} = \begin{bmatrix} 0 & \mathrm{z}^{\mathrm{c}} & -\mathrm{y}^{\mathrm{c}} \\ -\mathrm{z}^{\mathrm{c}} & 0 & \mathrm{x}^{\mathrm{c}} \\ \mathrm{y}^{\mathrm{c}} & -\mathrm{x}^{\mathrm{c}} & 0 \end{bmatrix}, \tag{2.17}$$

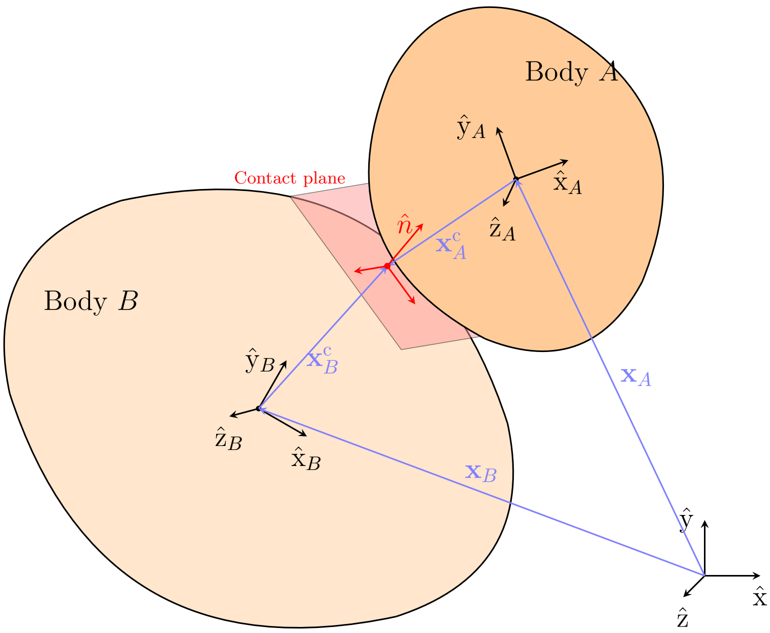

Figure 2.3: Local frames associated with the contact problem.

The absolute velocity and the contact impulse, respectively denoted by $\mathbf{u}$ and $\mathbf{r}$, can be expressed in the local frame as:

$$\mathbf{u} = \mathbf{H}^T \mathbf{v}, \tag{2.18}$$

$$\mathbf{p} = \mathbf{H}\mathbf{r}, \tag{2.19}$$

where $\mathbf{H}$ maps the global frame to the local frame at the contact point, defined as:

$$\mathbf{H} = \begin{bmatrix} \mathbf{I} \\ \mathbf{R} \end{bmatrix} \mathbf{B}, \qquad \mathbf{B} = \begin{bmatrix} \mathbf{n} & \mathbf{s} & \mathbf{t} \end{bmatrix}, \tag{2.20}$$

where $\mathbf{B}$ is change of basis matrix from the local frame to the global frame. It should be recall that the contact point and The transformation matrix $\mathbf{H}$ are not known a priori as they depends on the bodies configuration.

Over a singleton $\{t^c\}$, the jump velocity at the contact point, Equation

(2.12), can be expressed in the local frame as:

$$\mathbf{M}(\mathbf{v}^+ - \mathbf{v}^-) = \mathbf{p}, \tag{2.21}$$

$$\mathbf{v}^+ - \mathbf{v}^- = \mathbf{M}^{-1}\mathbf{p}, \tag{2.22}$$

$$\mathbf{H}^T(\mathbf{v}^+ - \mathbf{v}^-) = \mathbf{H}^T\mathbf{M}^{-1}\mathbf{H}\mathbf{r}, \tag{2.23}$$

$$\mathbf{u}^+ - \mathbf{u}^- = \mathbf{H}^T\mathbf{M}^{-1}\mathbf{H}\mathbf{r}, \tag{2.24}$$

It is convenient to introduce the Delassus operator $\mathbf{W}$ which describes the change of velocity at the contact point due to the contact impulse,

$$\mathbf{u}^+ - \mathbf{u}^- = \mathbf{W}\mathbf{r}, \qquad \mathbf{W} = \mathbf{H}^T\mathbf{M}^{-1}\mathbf{H}, \tag{2.25}$$

At the contact point between two bodies A and B, the dynamics at the contact point is expressed as:

$$\mathbf{u}_A^+ = \mathbf{u}_A^- + \mathbf{W}_A\mathbf{r}, \qquad \mathbf{W}_A = \mathbf{H}_A^T\mathbf{M}_A^{-1}\mathbf{H}_A \tag{2.26}$$

$$\mathbf{u}_B^+ = \mathbf{u}_B^- - \mathbf{W}_B\mathbf{r}, \qquad \mathbf{W}_B = \mathbf{H}_B^T\mathbf{M}_B^{-1}\mathbf{H}_B \tag{2.27}$$

Let $\delta\mathbf{u} = \mathbf{u}_A - \mathbf{u}_B$ be the relative velocity at the contact point. The dynamics at the contact point is:

$$\delta\mathbf{u}^+ = \delta\mathbf{u}^- + \mathbf{W}\mathbf{r}, \qquad \mathbf{W} = \mathbf{W}_A + \mathbf{W}_B \tag{2.28}$$

Regarding this equation, both the contact impulse $\mathbf{r}$ and the relative velocity $\delta\mathbf{u}^+$ are unknown. In three-dimensional space, six unknowns have to be solved, the contact dynamics, Equation (2.28) only provides three equations. To close the system, non-overlapping conditions are imposed at the contact point and constitutive laws are introduced to model tangential reactions with inelastic collisions.

2.2.2 Signorini's Condition

Non-smooth methods seek to prevent overlapping between two bodies. This is why they are also referred as hard-sphere methods. To ensure non-overlapping, the gap, Equation (2.13), is set to be non-negative

$$g(t) \geq 0, \tag{2.29}$$

This condition is referred as the unilateral constraint. As two bodies are close to one another without contact, the gap is positive and the normal contact impulse is zero. When the two bodies are in contact, the gap is zero and the normal contact impulse is positive. This situation is referred as the Signorini's condition:

$$g(t) \geq 0, \qquad \text{(Impenetrability)}, \tag{2.30}$$
$$\mathrm{r}_n(t) \geq 0, \qquad \text{(No attraction)}, \tag{2.31}$$
$$\mathrm{r}_n(t)g(t) = 0, \qquad \text{(Signorini's condition)}, \tag{2.32}$$

where r_n is the normal contact impulse. Figure 2.4a illustrates the Signorini's condition.

2.2.3 Frictional Contact Law

In order to fully describe the contact dynamics, constitutive laws are required to model the contact forces. Inelastic shock and Coulomb's friction law are the ones considered in this work. The inelastic shock states that if a contact occurs, the contact normal velocity vanishes after the contact,

$$g(t) = 0 \Rightarrow \mathrm{r}_n(t) \geq 0, \qquad \delta \mathrm{u}_n^+ = 0. \tag{2.33}$$

Coulomb's friction law states that the tangential contact impulse is opposite to the tangential velocity at the contact point and that its magnitude belongs to the friction cone with a friction coefficient μ. Figure 2.4b illustrates the Coulomb's friction law for a two-dimensional system. In the contact frame, the Coulomb's friction law can be expressed as:

$$\|\mathbf{r}_t\| \leq \mu \mathrm{r}_n, \tag{2.34}$$
$$\left\|\delta \mathbf{u}_t^+\right\| \neq 0 \Rightarrow \mathbf{r}_t = -\mu \mathrm{r}_n \frac{\delta \mathbf{u}_t^+}{\left\|\delta \mathbf{u}_t^+\right\|}. \tag{2.35}$$

where $\mathbf{r}_t$ is the tangential contact impulse and $\delta \mathbf{u}_t^+$ is the tangential velocity at the contact point defined as:

$$\mathbf{r}_t = \mathbf{r} - \mathrm{r}_n \mathbf{n}, \qquad \delta \mathbf{u}_t^+ = \delta \mathbf{u}^+ - \delta \mathrm{u}_n^+ \mathbf{n}. \tag{2.36}$$

2.2.4 A Brief Summary

For a given contact point, the contact impulse and the relative velocity are determined to satisfy the contact dynamics, the Signorini condition (impenetrability), Coulomb's friction law (Coulomb's cone and slipping), and the inelastic impact condition (no restitution).

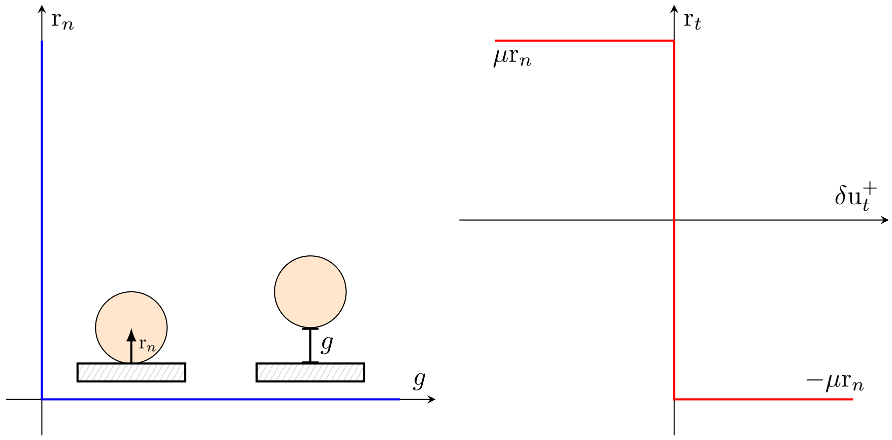

(a) Signorini's condition.

(b) Coulomb's friction law.

$$
\begin{aligned}
&\delta\mathbf{u}^+ = \delta\mathbf{u}^- + \mathbf{W}\mathbf{r}, && \text{(Contact Dynamics)}\\
&g(t) \geq 0, && \text{(Impenetrability)},\\
&\mathrm{r}_n(t) \geq 0, && \text{(No attraction)},\\
&\mathrm{r}_n(t)g(t) = 0, && \text{(Signorini's condition)},\\
&g(t) = 0 \Rightarrow \mathrm{r}_n(t) \geq 0, \delta\mathrm{u}_n^+ = 0, && \text{(No restitution)}.\\
&\|\mathbf{r}_t\| \leq \mu\mathrm{r}_n, && \text{(Coulomb's cone)}\\
&\left\|\delta\mathbf{u}_t^+\right\| \neq 0 \Rightarrow \mathbf{r}_t = -\mu\mathrm{r}_n\frac{\delta\mathbf{u}_t^+}{\left\|\delta\mathbf{u}_t^+\right\|}, && \text{(Slipping)}.
\end{aligned}
\tag{2.37}
$$

The complete contact problem is inherently nonlinear, so finding a solution is not trivial. Fortunately, in two-dimensional problems, an explicit solution can often be obtained using a graphical interpretation of the contact laws. This allows for a direct construction of the contact impulse that satisfies the Signorini condition, Coulomb's friction law, and the inelastic impact condition. However, in three-dimensional configurations, the contact space becomes more complex, and an iterative procedure is typically required to find the correct contact impulse at each contact point. The following paragraph illustrates how the contact solution can be obtained explicitly in a bidimensional problem.

A bidimensional example — Let us assume an active contact between two bidimensional bodies, *i.e.* the gap is zero. The contact solution is the relative velocity and the contact impulse such that both the contact dynamics and the Coulomb's friction law are satisfied. The solution can be found graphically by determining the intersection between the contact dynamics and the

Coulomb friction law, as illustrated in Figure 2.5. To discuss this intersection, we introduce the stick impulse, which is the impulse such that the relative velocity vanishes:

$$\mathbf{r}^{\text{stick}} = -\mathbf{W}^{-1}\delta\mathbf{u}^{-}. \tag{2.38}$$

If the stick solution is inside the friction cone, then the contact is in stick mode and the contact impulse is equal to the stick impulse. If the stick solution is outside the friction cone, then the contact is in slip mode and the contact impulse is equal to the boundary of the friction cone. The sign of the stick tangential impulse determines the direction of the slip either forward or backward,

$$\text{if } \mathrm{r}_t^{\text{stick}} - \mu\mathrm{r}_n^{\text{stick}} < 0, \quad \text{then } \mathrm{r}_t = -\mu\mathrm{r}_n \tag{2.39}$$

$$\text{if } \mathrm{r}_t^{\text{stick}} + \mu\mathrm{r}_n^{\text{stick}} > 0, \quad \text{then } \mathrm{r}_t = \mu\mathrm{r}_n \tag{2.40}$$

Finally, the tangential contact impulse is injected into the contact dynamics, a 2×2 system of linear equations is obtained,

$$\begin{bmatrix} 0 \\ \delta\mathrm{u}_t^{+} \end{bmatrix} = \begin{bmatrix} \mathrm{W}_{nn} & \mathrm{W}_{nt} \\ \mathrm{W}_{tn} & \mathrm{W}_{tt} \end{bmatrix} \begin{bmatrix} \mathrm{r}_n \\ \mathrm{r}_t \end{bmatrix} + \begin{bmatrix} \delta\mathrm{u}_n^{-} \\ \delta\mathrm{u}_t^{-} \end{bmatrix}. \tag{2.41}$$

From this system, the tangential velocity and the normal impulse can be isolated and thus, the contact problem has been fully solved.

In this section, we present the Non-Smooth Contact Dynamics (NSCD) framework for modelling a single collision between two bodies. The dynamics are described in a local frame associated with the contact point. To ensure non-penetration at all times, Signorini's condition is applied. To close the system of equations, constitutive laws are introduced to model the contact forces–specifically, the inelastic impact condition and Coulomb's friction law. However, in practical scenarios, multiple contacts typically occur within a single time step. Resolving these interactions requires solving a global multi-contact problem. The following section details the iterative algorithm used to compute a consistent set of contact impulses that satisfies all constraints.

2.3 When One Contact Isn't Enough

In most realistic scenarios, multiple contacts occur simultaneously within a single time step. The objective is to determine a global contact impulse such that each local contact problem satisfies the conditions outlined in Equation (2.2.4).

Given that the current implementation is sequential, we assume contacts are resolved one after another. However, this resolution introduces a challenge: solving one contact updates the velocities of the involved bodies, which

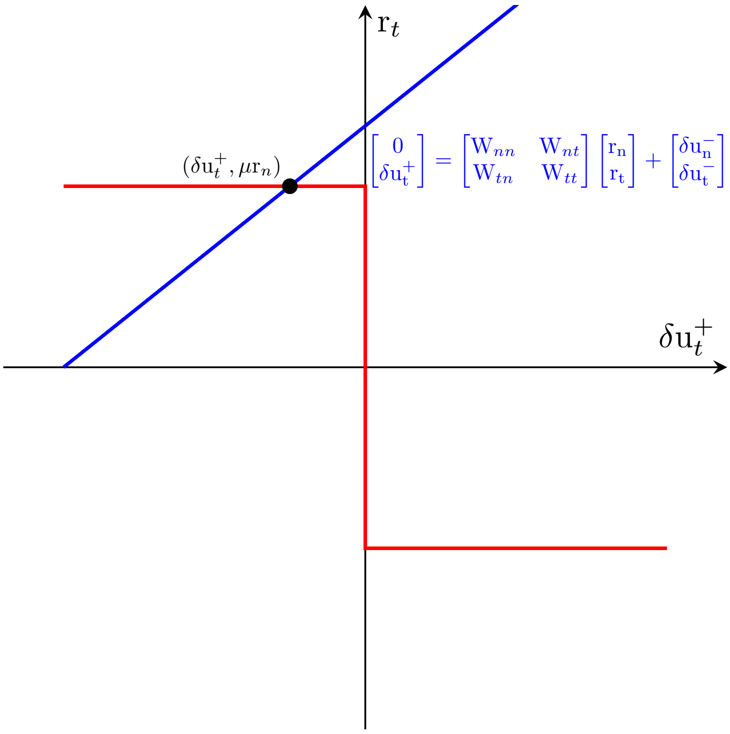

Figure 2.5: Coulomb's friction contact solution procedure.

may, in turn, affect other previously solved contacts. To address this coupling, iterative schemes are employed to achieve convergence. Common methods include the *Nonlinear Gauss–Seidel* algorithm [40, 77] and *Conjugate Gradient methods* [78]. Optimisation-based approaches such as the *Accelerated Gradient Scheme* [39] have also shown promise, offering efficient convergence properties.

In this work, we adopt the Nonlinear Gauss–Seidel method to solve the multi-contact problem. Algorithm 2 summarizes the procedure. Let us assume that all detected contacts are stored in a list $\mathcal{C}$. The algorithm begins with an initial guess for the contact impulses, denoted $\mathbf{r}_0$. It then iteratively loops through each contact in $\mathcal{C}$. For each contact, the previously applied contact impulse is removed from the bodies. Then the local contact problem is solved using Equation (2.2.4), yielding an updated contact impulse. This contact impulse is then re-applied to the bodies involved in the contact. To assess local convergence, the displacement at the contact point is compared to that from the previous iteration. If the change is below a specified tolerance ξ, the contact is considered to have converged and the previous contact impulse is applied. The algorithm terminates once all contacts satisfy the local convergence criterion.

Algorithm 2: Non-Linear Gauss Seidel Loop.

Data: Initial guess $\mathbf{r}_0$
k = 0;
converged = False;
while *not converged* **do**
  for *Each contact* $\alpha \in \mathcal{C}$ **do**
    k += 1;
    $\mathbf{v}_0^\alpha, \mathbf{v}_1^\alpha \rightarrow$ Unapply the contact impulse $\mathbf{r}_{k-1}^\alpha$;
    $\delta\mathbf{u}_k^\alpha, \mathbf{r}_k^\alpha \rightarrow$ Solve the local contact problem;
    $\mathbf{v}_0^\alpha, \mathbf{v}_1^\alpha \rightarrow$ Apply the contact impulse $\mathbf{r}_k^\alpha$;
    if $\left\|\delta\mathbf{u}_k^\alpha - \delta\mathbf{u}_{k-1}^\alpha\right\|\Delta t < \xi$ **then**
      converged = True;
      $\mathbf{v}_0^\alpha, \mathbf{v}_1^\alpha \rightarrow$ Unapply the contact impulse $\mathbf{r}_k^\alpha$;
      $\mathbf{v}_0^\alpha, \mathbf{v}_1^\alpha \rightarrow$ Apply the contact impulse $\mathbf{r}_{k-1}^\alpha$;
    end
  end
end

Optimisation As observed in the previously described algorithm, even if only a few contacts require additional iterations to converge, the algorithm continues to loop over all contacts at each step. This inefficiency has been addressed by introducing a queue to manage contact resolution more effectively. Initially, all detected contacts are inserted into the queue. We then iterate through the queue, solving one contact at a time. If a contact fails to converge, it is reinserted back into the queue, along with all contacts involving the same bodies. This strategy focuses computational effort on unresolved contacts and their immediate neighbors, which are most likely to be affected. Consequently, the algorithm becomes more efficient by dynamically adapting its focus to the regions of the system where convergence has not yet been achieved.

Conclusion

In this chapter, we present the Non-Smooth Contact Dynamics (NSCD) framework for modelling contact interactions between rigid bodies. This method treats contact events as instantaneous and discontinuous, represented through impulses. The NSCD approach enables the robust simulation of systems with many simultaneous contacts, such as granular materials.

Algorithm 3 summarises the overall procedure for the NSCD method. The free velocity $\mathbf{v}^-$ is computed based on the external forces acting on the bodies. Potential contacts are detected, and the contact impulse is computed using the Nonlinear Gauss–Seidel algorithm. Finally, the bodies positions are updated based on the computed velocities. The time step Δt must be chosen to ensure stability in the explicit force computation and to allow for an accurate contact detection.

Algorithm 3: NSCD Overview.

Require: $\mathbf{q}^n, \mathbf{v}^n, \mathbf{f}_e^n, \Delta t$

$\mathbf{v}^-$	$\leftarrow$	$\mathbf{v}^n + \Delta t \mathbf{f}_e^n$
$\mathcal{C}$	$\leftarrow$	Contact Detection
$\mathbf{p}^{n+1}, \mathbf{v}^{n+1}$	$\leftarrow$	NonLinear Gauss-Seidel
$\mathbf{q}^{n+1}$	$\leftarrow$	Update the bodies position

In the next chapter, we turn our attention to the fluid phase representation and detail the coupling strategy between the fluid and solid phases.

Bibliography

[1] Jan K Marzinek, Roland G Huber, and Peter J Bond. “Multiscale modelling and simulation of viruses”. In: *Current opinion in structural biology* 61 (2020), pp. 146–152. DOI: 10.1016/j.sbi.2019.12.019.

[2] Johannes Voß and Raphael Wittkowski. “On the shape-dependent propulsion of nano and microparticles by traveling ultrasound waves”. In: *Nanoscale Advances* 2.9 (2020), pp. 3890–3899. DOI: 10.1039/D0NA00099J.

[3] Yiwu Zong and Kun Zhao. “Manipulation of self-assembled structures by shape-designed polygonal colloids in 2D”. In: *Current Opinion in Solid State and Materials Science* 26.6 (2022), p. 101022.

[4] Xi Luo et al. “A review of analytical methods and models used in atmospheric microplastic research”. In: *Science of the Total Environment* 828 (2022), p. 154487.

[5] Jonathan B Freund. “Numerical simulation of flowing blood cells”. In: *Annual review of fluid mechanics* 46.1 (2014), pp. 67–95.

[6] Guilhem Mollon and Jidong Zhao. “Generating realistic 3D sand particles using Fourier descriptors”. In: *Granular Matter* 15 (2013), pp. 95–108.

[7] Guillaume Piton et al. “Debris flows, boulders and constrictions: a simple framework for modeling jamming, and its consequences on outflow”. In: *Journal of Geophysical Research: Earth Surface* 127.5 (2022).

[8] Thomas Rackow et al. “A simulation of small to giant A ntarctic iceberg evolution: Differential impact on climatology estimates”. In: *Journal of Geophysical Research: Oceans* 122.4 (2017), pp. 3170–3190.

[9] Fabio Ferrari, Michèle Lavagna, and Emmanuel Blazquez. “A parallel-GPU code for asteroid aggregation problems with angular particles”. In: *Monthly Notices of the Royal Astronomical Society* 492.1 (2020), pp. 749–761.

[10] Yoël Forterre and Olivier Pouliquen. “Physics of particulate flows: From sand avalanche to active suspensions in plants”. In: *Comptes Rendus. Physique* 19.5 (2018), pp. 271–284.

[11] Élisabeth Guazzelli and Olivier Pouliquen. "Rheology of dense granular suspensions". In: *Journal of Fluid Mechanics* 852 (2018), P1.

[12] Farhang Radjai, Frédéric Dubois, et al. *Modélisation numérique discrète des matériaux granulaires*. Hermès science, 2010.

[13] Jidong Zhao, Shiwei Zhao, and Stefan Luding. "The role of particle shape in computational modelling of granular matter". In: *Nature Reviews Physics* 5.9 (2023), pp. 505–525.

[14] Brian Miller, Corey O'Hern, and RP Behringer. "Stress fluctuations for continuously sheared granular materials". In: *Physical Review Letters* 77.15 (1996), p. 3110.

[15] Daniel Howell, Robert P Behringer, and Christian Veje. "Stress fluctuations in a 2D granular Couette experiment: a continuous transition". In: *Physical Review Letters* 82.26 (1999), p. 5241.

[16] CT Veje, Daniel W Howell, and RP Behringer. "Kinematics of a two-dimensional granular Couette experiment at the transition to shearing". In: *Physical Review E* 59.1 (1999), p. 739.

[17] Lhassan Amarsid et al. "Viscoinertial regime of immersed granular flows". In: *Physical Review E* 96.1 (2017), p. 012901.

[18] Stany Gallier et al. "Rheology of Sheared Suspensions of Rough Frictional Particles". In: *Journal of Fluid Mechanics* 757 (Oct. 2014), pp. 514–549. ISSN: 0022-1120, 1469-7645. DOI: 10.1017/jfm.2014.507.

[19] François Boyer, Élisabeth Guazzelli, and Olivier Pouliquen. "Unifying suspension and granular rheology". In: *Physical review letters* 107.18 (2011), p. 188301.

[20] Thanh Trung Vo et al. "Additive rheology of complex granular flows". In: *Nature communications* 11.1 (2020), p. 1476.

[21] David Cantor et al. "Rheology and structure of polydisperse three-dimensional packings of spheres". In: *Physical Review E* 98.5 (2018), p. 052910.

[22] George Gabriel Stokes et al. "On the effect of the internal friction of fluids on the motion of pendulums". In: (1851).

[23] J. M. DallaValle and Alexander Klemin. *Micromeritics: The Technology of the Particles*. New York ; Chicago: Pitman Publishing Corporation, 1943.

[24] R. Di Felice. "The Voidage Function for Fluid-Particle Interaction Systems". In: *International Journal of Multiphase Flow* 20.1 (Feb. 1994), pp. 153–159. ISSN: 0301-9322. DOI: 10.1016/0301-9322(94)90011-6.

[25] DA Huerta et al. "Archimedes' principle in fluidized granular systems". In: *Physical Review E—Statistical, Nonlinear, and Soft Matter Physics* 72.3 (2005), p. 031307.

[26] Heinrich G Magnus. *Über die Abweichung der Geschosse*. Druckerei der Königlichen Akademie der Wissenschaften, 1853.

[27] Thorsten Kray, Jörg Franke, and Wolfram Frank. "Magnus effect on a rotating sphere at high Reynolds numbers". In: *Journal of wind engineering and industrial aerodynamics* 110 (2012), pp. 1–9.

[28] Philip Geoffrey Saffman. "The lift on a small sphere in a slow shear flow". In: *Journal of fluid mechanics* 22.2 (1965), pp. 385–400.

[29] Xu Zheng and Zhanhua Silber-Li. "The influence of Saffman lift force on nanoparticle concentration distribution near a wall". In: *Applied physics letters* 95.12 (2009).

[30] Christopher Earls Brennen. "A review of added mass and fluid inertial forces". In: *Naval Civil Engineering Laboratory* (1982).

[31] Louis Landweber and Ali Shahshahan. "Added masses and forces on two bodies approaching central impact in an inviscid fluid". In: *Journal of ship research* 36.02 (1992), pp. 99–122.

[32] Alfred Barnard Basset. *A treatise on hydrodynamics: with numerous examples*. Vol. 2. Deighton, Bell and Company, 1888.

[33] Patricio A Moreno-Casas and Fabian A Bombardelli. "Computation of the Basset force: recent advances and environmental flow applications". In: *Environmental Fluid Mechanics* 16 (2016), pp. 193–208.

[34] GK Batchelor and JT0246 Green. "The determination of the bulk stress in a suspension of spherical particles to order c2". In: *Journal of Fluid Mechanics* 56.3 (1972), pp. 401–427.

[35] Irvin M Krieger and Thomas J Dougherty. "A mechanism for non-Newtonian flow in suspensions of rigid spheres". In: *Transactions of the Society of Rheology* 3.1 (1959), pp. 137–152.

[36] Peter A Cundall and Otto DL Strack. "A discrete numerical model for granular assemblies". In: *geotechnique* 29.1 (1979), pp. 47–65.

[37] Nicolin Govender. "Study on the effect of grain morphology on shear strength in granular materials via GPU based discrete element method simulations". In: *Powder Technology* 387 (2021), pp. 336–347.

[38] Frédéric Dubois, Vincent Acary, and Michel Jean. "The Contact Dynamics Method: A Nonsmooth Story". In: *Comptes Rendus Mécanique*. The Legacy of Jean-Jacques Moreau in Mechanics / L'héritage de Jean-Jacques Moreau En Mécanique 346.3 (Mar. 2018), pp. 247–262. ISSN: 1631-0721. DOI: 10.1016/j.crme.2017.12.009.

[39] Hammad Mazhar et al. “Using Nesterov’s method to accelerate multibody dynamics with friction and contact”. In: *ACM Transactions on Graphics (TOG)* 34.3 (2015), pp. 1–14.

[40] Franck Jourdan, Pierre Alart, and Michel Jean. “A Gauss-Seidel like algorithm to solve frictional contact problems”. In: *Computer methods in applied mechanics and engineering* 155.1-2 (1998), pp. 31–47.

[41] N Bessonov et al. “Numerical Modelling of Cell Distribution in Blood-Flow”. In: *Mathematical Modelling of Natural Phenomena* 9.6 (2014), pp. 69–84.

[42] Thomas JR Hughes, Wing Kam Liu, and Thomas K Zimmermann. “Lagrangian-Eulerian finite element formulation for incompressible viscous flows”. In: *Computer methods in applied mechanics and engineering* 29.3 (1981), pp. 329–349.

[43] Eugenio Oñate et al. “The particle finite element method—an overview”. In: *International Journal of Computational Methods* 1.02 (2004), pp. 267–307.

[44] C.S. Peskin. “Numerical analysis of blood flow in the heart”. In: *Journal of computational physics* 25.3 (1977), pp. 220–252.

[45] Erik Burman and Miguel A Fernández. “An unfitted Nitsche method for incompressible fluid–structure interaction using overlapping meshes”. In: *Computer Methods in Applied Mechanics and Engineering* 279 (2014), pp. 497–514.

[46] Joseph J Monaghan. “Smoothed particle hydrodynamics and its diverse applications”. In: *Annual Review of Fluid Mechanics* 44.1 (2012), pp. 323–346.

[47] AA Mohamad. *Lattice boltzmann method*. Vol. 70. Springer, 2011.

[48] T. B. Anderson and Roy Jackson. “Fluid Mechanical Description of Fluidized Beds. Equations of Motion”. In: *Industrial & Engineering Chemistry Fundamentals* 6.4 (Nov. 1967), pp. 527–539. ISSN: 0196-4313. DOI: 10.1021/i160024a007.

[49] Jesse Capecelatro and Olivier Desjardins. “An Euler–Lagrange Strategy for Simulating Particle-Laden Flows”. In: *Journal of Computational Physics* 238 (Apr. 2013), pp. 1–31. ISSN: 00219991. DOI: 10.1016/j.jcp.2012.12.015.

[50] Toni El Geitani, Shahab Golshan, and Bruno Blais. “A High-Order Stabilized Solver for the Volume Averaged Navier-Stokes Equations”. In: *International Journal for Numerical Methods in Fluids* 95.6 (2023), pp. 1011–1033. ISSN: 1097-0363. DOI: 10.1002/fld.5182.

[51] ZY Zhou et al. “Discrete particle simulation of particle–fluid flow: model formulations and their applicability”. In: *Journal of Fluid Mechanics* 661 (2010), pp. 482–510.

[52] Zekun Wang, Yujun Teng, and Moubin Liu. “A semi-resolved CFD–DEM approach for particulate flows with kernel based approximation and Hilbert curve based searching strategy”. In: *Journal of Computational Physics* 384 (2019), pp. 151–169.

[53] Toni El Geitani and Bruno Blais. “Quadrature-centered averaging scheme for accurate and continuous void fraction calculation in computational fluid dynamics–discrete element method simulations”. In: *Industrial & Engineering Chemistry Research* 62.12 (2023), pp. 5394–5407.

[54] Matthieu Constant. “Simulations of immersed granular flows using an unresolved FEM-DEM model”. PhD thesis. UCL-Université Catholique de Louvain, 2020.

[55] Matthieu Constant et al. “Implementation of an Unresolved Stabilised FEM–DEM Model to Solve Immersed Granular Flows”. In: *Computational Particle Mechanics* (Sept. 2018). ISSN: 2196-4378, 2196-4386. DOI: 10.1007/s40571-018-0209-4.

[56] M. Constant et al. “Simulation of Air Invasion in Immersed Granular Beds with an Unresolved FEM–DEM Model”. In: *Computational Particle Mechanics* (Sept. 2020). ISSN: 2196-4386. DOI: 10.1007/s40571-020-00351-4.

[57] M. Constant et al. “Numerical investigation of the density sorting of grains using water jigging”. In: *Powder Technology* 393 (2021), pp. 705–721.

[58] Nathan Coppin. “Numerical methods for flows of immersed grain clusters”. PhD thesis. UCL-Université Catholique de Louvain, 2023.

[59] Nathan Coppin et al. “Numerical Analysis of the Drag on a Rigid Body in an Immersed Granular Flow”. In: *Particles 2021*. Hamburg, 2021.

[60] Nathan Coppin et al. “Collapse dynamics of two-dimensional dry and immersed granular columns of elongated grains”. In: *Physical Review Fluids* 8.9 (2023), p. 094303.

[61] Fangye Lin et al. *Deep Spontaneous Penetration of a Water Droplet into Hot Granular Materials*. Preprint. In Review, Dec. 2020. DOI: 10.21203/rs.3.rs-103868/v1.

[62] Alessandro Franci et al. “PFEM–DEM for particle-laden flows with free surface”. In: *Computational Particle Mechanics* 7 (2020), pp. 101–120.

[63] Wladimir Sarlin et al. “Nonlinear regimes of tsunami waves generated by a granular collapse”. In: *Journal of Fluid Mechanics* 919 (2021), R6.

[64] Hermann M Fritz, Fahad Mohammed, and Jeseon Yoo. “Lituya Bay landslide impact generated mega-tsunami 50 th Anniversary”. In: *Tsunami Science four years after the 2004 Indian ocean tsunami: Part II: Observation and data analysis* (2009), pp. 153–175.

[65] Pierre Jop, Yoël Forterre, and Olivier Pouliquen. “A constitutive law for dense granular flows”. In: *Nature* 441.7094 (2006), pp. 727–730.

[66] Ken Kamrin and Georg Koval. “Nonlocal constitutive relation for steady granular flow”. In: *Physical review letters* 108.17 (2012), p. 178301.

[67] Olivier Pouliquen et al. “Flow of dense granular material: towards simple constitutive laws”. In: *Journal of Statistical Mechanics: Theory and Experiment* 2006.07 (2006), P07020.

[68] Olivier Ozenda, Pierre Saramito, and Guillaume Chambon. “Shear–induced migration in concentrated suspensions: particle mass conservation, contact pressure and jamming”. In: *Journal of Non-Newtonian Fluid Mechanics* 304 (2022), p. 104805.

[69] John G Rosser et al. “Investigation of Jamming Phenomenon in a Direct Reduction Furnace Pellet Feed System Using the Discrete Element Method”. In: *Dynamics* 3.4 (2023), pp. 711–736.

[70] Federico A Tavarez and Michael E Plesha. “Discrete element method for modelling solid and particulate materials”. In: *International journal for numerical methods in engineering* 70.4 (2007), pp. 379–404.

[71] ZX Yang, J Yang, and LZ Wang. “On the influence of inter-particle friction and dilatancy in granular materials: a numerical analysis”. In: *Granular matter* 14 (2012), pp. 433–447.

[72] Kevin Francis Malone and Bao Hua Xu. “Determination of contact parameters for discrete element method simulations of granular systems”. In: *Particuology* 6.6 (2008), pp. 521–528.

[73] Michel Jean. “The non-smooth contact dynamics method”. In: *Computer methods in applied mechanics and engineering* 177.3-4 (1999), pp. 235–257.

[74] Frédéric Dubois, Vincent Acary, and Michel Jean. “The Contact Dynamics method: A nonsmooth story”. In: *Comptes Rendus Mécanique* 346.3 (2018), pp. 247–262.

[75] Michel Jean and Jean Jacques Moreau. “Unilaterality and dry friction in the dynamics of rigid body collections”. In: *1st Contact Mechanics International Symposium*. 1992, pp. 31–48.

[76] Jean J Moreau. “Unilateral contact and dry friction in finite freedom dynamics”. In: *Nonsmooth mechanics and Applications*. Springer, 1988, pp. 1–82.

[77] Mihai Anitescu and Alessandro Tasora. "An iterative approach for cone complementarity problems for nonsmooth dynamics". In: *Computational Optimization and Applications* 47.2 (2010), pp. 207–235.

[78] Mathieu Renouf and Pierre Alart. "Conjugate gradient type algorithms for frictional multi-contact problems: applications to granular materials". In: *Computer Methods in Applied Mechanics and Engineering* 194.18-20 (2005), pp. 2019–2041.

[79] Efstathios E Michaelides, Martin Sommerfeld, and Berend van Wachem. *Multiphase flows with droplets and particles*. CRC Press, 2022.

[80] CB Rogers and JK Eaton. "The effect of small particles on fluid turbulence in a flat-plate, turbulent boundary layer in air". In: *Physics of Fluids A: Fluid Dynamics* 3.5 (1991), pp. 928–937.

[81] Clayton T Crowe. "On models for turbulence modulation in fluid–particle flows". In: *International Journal of Multiphase Flow* 26.5 (2000), pp. 719–727.

[82] Albert Einstein. "Eine neue bestimmung der moleküldimensionen". PhD thesis. ETH Zurich, 1905.

[83] DZ Zhang and A Prosperetti. "Momentum and energy equations for disperse two-phase flows and their closure for dilute suspensions". In: *International journal of multiphase flow* 23.3 (1997), pp. 425–453.

[84] Neelesh A Patankar and Daniel D Joseph. "Modeling and numerical simulation of particulate flows by the Eulerian–Lagrangian approach". In: *International journal of multiphase flow* 27.10 (2001), pp. 1659–1684.

[85] Alberto Di Renzo and Francesco Paolo Di Maio. "Homogeneous and bubbling fluidization regimes in DEM–CFD simulations: hydrodynamic stability of gas and liquid fluidized beds". In: *Chemical engineering science* 62.1-2 (2007), pp. 116–130.

[86] Ivo Babuška. "The finite element method with Lagrangian multipliers". In: *Numerische Mathematik* 20.3 (1973), pp. 179–192.

[87] Franco Brezzi and Juhani Pitkäranta. "On the stabilization of finite element approximations of the Stokes equations". In: *Efficient solutions of elliptic systems*. Springer, 1984, pp. 11–19.

[88] T.E. Tezduyar et al. "Incompressible flow computations with stabilized bilinear and linear equal-order interpolation velocity-pressure elements". In: *Computer Methods in Applied Mechanics and Engineering* 95 (1992), pp. 221–242.

[89] A. N. Brooks and T. J. R. Hughes. "Streamline upwind/Petrov-Galerkin formulations for convection dominated flows with particular emphasis on the incompressible Navier-Stokes equations". In: *Computer methods in applied mechanics and engineering* 32.1-3 (1982), pp. 199–259.

[90] T. E. Tezduyar and Y. Osawa. "Finite element stabilization parameters computed from element matrices and vectors". In: *Computer Methods in Applied Mechanics and Engineering* 190.3-4 (2000), pp. 411–430.

[91] Chuan Miao Chen and Vidar Thomée. "The lumped mass finite element method for a parabolic problem". In: *The ANZIAM Journal* 26.3 (1985), pp. 329–354.

[92] Daniel A. Clarke et al. "Investigation of Void Fraction Schemes for Use with CFD-DEM Simulations of Fluidized Beds". In: *Industrial & Engineering Chemistry Research* 57.8 (Feb. 2018), pp. 3002–3013. ISSN: 0888-5885. DOI: 10.1021/acs.iecr.7b04638.

[93] Zekun Wang and Moubin Liu. "Semi-resolved CFD–DEM for thermal particulate flows with applications to fluidized beds". In: *International Journal of Heat and Mass Transfer* 159 (2020), p. 120150.

[94] Thomas Engels et al. "Numerical simulation of fluid–structure interaction with the volume penalization method". In: *Journal of Computational Physics* 281 (2015), pp. 96–115.

[95] Ramakrishnan Thirumalaisamy and Amneet Pal Singh Bhalla. "A consistent, volume preserving, and adaptive mesh refinement–based framework for modeling non–isothermal gas–liquid–solid flows with phase change". In: *International Journal of Multiphase Flow* 183 (2025).

[96] A Piquet, Olivier Roussel, and Abdellah Hadjadj. "A comparative study of Brinkman penalization and direct-forcing immersed boundary methods for compressible viscous flows". In: *Computers & Fluids* 136 (2016), pp. 272–284.

[97] Jan Ludvig Vinningland et al. "Experiments and simulations of a gravitational granular flow instability". In: *Physical Review E—Statistical, Nonlinear, and Soft Matter Physics* 76.5 (2007), p. 051306.

[98] Geoffrey Ingram Taylor. "The instability of liquid surfaces when accelerated in a direction perpendicular to their planes. I". In: *Proceedings of the Royal Society of London. Series A. Mathematical and Physical Sciences* 201.1065 (1950), pp. 192–196.

[99] Jan Ludvig Vinningland et al. "Size invariance of the granular Rayleigh-Taylor instability". In: *Physical Review E—Statistical, Nonlinear, and Soft Matter Physics* 81.4 (2010), p. 041308.

[100] Sige Peng and John D Rice. "Measuring critical gradients for soil loosening and initiation of backward erosion-piping mechanism". In: *Journal of Geotechnical and Geoenvironmental Engineering* 146.8 (2020), p. 04020069.

[101] Kak Namkoong, Jung Yul Yoo, and Hyoung G Choi. "Numerical analysis of two-dimensional motion of a freely falling circular cylinder in an infinite fluid". In: *Journal of Fluid Mechanics* 604 (2008), pp. 33–53.

[102] Zhi-Gang Feng and Efstathios E Michaelides. "The immersed boundary-lattice Boltzmann method for solving fluid–particles interaction problems". In: *Journal of computational physics* 195.2 (2004), pp. 602–628.

[103] L Wang, ZL Guo, and JC3198060 Mi. "Drafting, kissing and tumbling process of two particles with different sizes". In: *Computers & Fluids* 96 (2014), pp. 20–34.

[104] Sudeshna Ghosh and Manish Kumar. "Study of drafting, kissing and tumbling process of two particles with different sizes and densities using immersed boundary method in a confined medium". In: *Applied Mathematics and Computation* 386 (2020), p. 125411.

[105] Prabir Basu. *Circulating Fluidized Bed Boilers: Design, Operation and Maintenance*. Cham: Springer International Publishing, 2015. ISBN: 978-3-319-06172-6 978-3-319-06173-3. DOI: 10.1007/978-3-319-06173-3.

[106] Chanchal Loha et al. "ChemInform Abstract: Advances in Mathematical Modeling of Fluidized Bed Gasification". In: *Renewable and Sustainable Energy Reviews* 40 (Dec. 2014), pp. 688–715. DOI: 10.1016/j.rser.2014.07.199.

[107] David Quéré. "Leidenfrost Dynamics". In: *Annual Review of Fluid Mechanics* 45.1 (Jan. 2013), pp. 197–215. ISSN: 0066-4189, 1545-4479. DOI: 10.1146/annurev-fluid-011212-140709.

[108] Lucia Rueda Villegas et al. "A Ghost Fluid/Level Set Method for Boiling Flows and Liquid Evaporation: Application to the Leidenfrost Effect". In: *Journal of Computational Physics* 316 (July 2016), pp. 789–813. ISSN: 0021-9991. DOI: 10.1016/j.jcp.2016.04.031.

[109] *A High-order Stabilized Solver for the Volume Averaged Navier-Stokes Equations - Geitani - 2023 - International Journal for Numerical Methods in Fluids - Wiley Online Library*.

[110] Khuram Walayat et al. "An Efficient Multi-Grid Finite Element Fictitious Boundary Method for Particulate Flows with Thermal Convection". In: *International Journal of Heat and Mass Transfer* 126 (Nov. 2018), pp. 452–465. ISSN: 0017-9310. DOI: 10.1016/j.ijheatmasstransfer.2018.05.007.

[111] *CFD-DEM Simulation of Heat Transfer in Fluidized Beds: Model Verification, Validation, and Application | Elsevier Enhanced Reader*. DOI: 10.1016/j.ces.2018.12.031.

[112] WE Ranz. "Evaporation from Drops-I and-II". In: 48 (1952), pp. 141–146.

[113] I. C. Kemp, R. E. Bahu, and H. S. Pasley. "model development and experimental studies of vertical pneumatic conveying dryers". In: *DRYING TECHNOLOGY* (May 2007). ISSN: 1323-1340. DOI: 10.1080/07373939408961008.

[114] J Li and D.J Mason. "A Computational Investigation of Transient Heat Transfer in Pneumatic Transport of Granular Particles". In: *Powder Technology* 112.3 (Oct. 2000), pp. 273–282. ISSN: 00325910. DOI: 10.1016/S0032-5910(00)00302-8.

[115] N. Wakao and T. Funazkri. "Effect of Fluid Dispersion Coefficients on Particle-to-Fluid Mass Transfer Coefficients in Packed Beds: Correlation of Sherwood Numbers". In: *Chemical Engineering Science* 33.10 (Jan. 1978), pp. 1375–1384. ISSN: 0009-2509. DOI: 10.1016/0009-2509(78)85120-3.

[116] A. V. Patil, E. A. J. F. Peters, and J. A. M. Kuipers. "Comparison of CFD–DEM Heat Transfer Simulations with Infrared/Visual Measurements". In: *Chemical Engineering Journal* 277 (Oct. 2015), pp. 388–401. ISSN: 1385-8947. DOI: 10.1016/j.cej.2015.04.131.

[117] Farhang Radjaï and Frédéric Dubois. "Modélisation numérique discrète des matériaux granulaires". In: ().

[118] George Keith Batchelor and RW O'brien. "Thermal or Electrical Conduction through a Granular Material". In: *Proceedings of the Royal Society of London. A. Mathematical and Physical Sciences* 355.1682 (1977), pp. 313–333.

[119] M. Michael Yovanovich. "Thermal Contact Resistance across Elastically Deformed Spheres." In: *Journal of Spacecraft and Rockets* 4.1 (1967), pp. 119–122. ISSN: 0022-4650. DOI: 10.2514/3.28821.

[120] Adrian Bejan and Allan D. Kraus. *Heat Transfer Handbook*. John Wiley & Sons, June 2003. ISBN: 978-0-471-39015-2.

[121] Michel Henry et al. "Multiscale FEM-DEM model for spontaneous droplet digging in a hot granular bed". In: *International Journal of Heat and Mass Transfer* 241 (2025), p. 126755.

[122] Zhipeng Duan and Yuanyuan Duan. "Sphere Drag and Heat Transfer". In: *Scientific Reports* 5 (July 2015). DOI: 10.1038/srep12304.

[123] C Yu Wen. "Mechanics of Fluidization". In: *Fluid Particle Technology, Chem. Eng. Progress. Symposium Series* 62 (1966), pp. 100–111.

[124] James De Acetis and George Thodos. *Mass and Heat Transfer in Flow of Gases Through Spherical Packings*. Research-Article. May 2002. DOI: 10.1021/ie50612a026.

[125] Walter Komarnicky. “Effect of Packing Geometry on Heat and Mass Transfer in Stacked Beds of Spheres”. PhD thesis. University of British Columbia, 1956. DOI: 10.14288/1.0059067.

[126] G. F. Malling and George Thodos. “Analogy between Mass and Heat Transfer in Beds of Spheres: Contributions Due to End Effects”. In: *International Journal of Heat and Mass Transfer* 10.4 (Apr. 1967), pp. 489–498. ISSN: 0017-9310. DOI: 10.1016/0017-9310(67)90169-X.

[127] A. S. Gupta and G. Thodos. “Mass and heat transfer in the flow of fluids through fixed and fluidized beds of spherical particles”. In: *A.I.Ch.E. (Am. Inst. Chem. Engrs.) J.* Vol: 8 (Nov. 1962). DOI: 10.1002/aic.690080509.

[128] Charles R Wilke and OA Hougen. “Mass transfer in the flow of gases through granular solids extended to low modified Reynolds numbers”. In: *Trans. Am. Inst. Chem. Eng* 41.4 (1945), pp. 445–451.

[129] CN Satterfield. “Simultaneous Heat and Mass Transfer in a Duffusion-Controlled Chemical Reaction ; Part II : Studies in a Packed Bed”. In: *Chem. Eng. Prog.* 50 (1954), pp. 504–510.

[130] Jian Yang et al. “Experimental Analysis of Forced Convective Heat Transfer in Novel Structured Packed Beds of Particles”. In: *Chemical Engineering Science* 71 (Mar. 2012), pp. 126–137. ISSN: 0009-2509. DOI: 10.1016/j.ces.2011.12.005.

[131] John R Grace. “Shapes and velocities of single drops and bubbles moving freely through immisicible liquids”. In: *Trans. Inst. Chem. Eng.* 54 (1976), pp. 167–173.

[132] Charles Voivret et al. “Space-filling properties of polydisperse granular media”. In: *Physical Review E* 76.2 (2007), p. 021301.

[133] Fatima Zahra El Korchi, Frédéric Jamin, and Moulay Saïd El Youssoufi. “Etude Expérimentale à l’échelle Locale de La Coalescence de Ponts Capillaires Dans Les Sols Granulaires”. In: *35èmes Rencontres Universitaires de Génie Civil.* Actes Des 35èmes Rencontres Universitaires de Génie Civil. Nantes, France, May 2017.

[134] Steven N Ward. “Landslide tsunami”. In: *Journal of Geophysical Research: Solid Earth* 106.B6 (2001), pp. 11201–11215.

[135] Stéphane Abadie et al. “Numerical simulation of waves generated by landslides using a multiple-fluid Navier–Stokes model”. In: *Coastal engineering* 57.9 (2010), pp. 779–794.

[136] Cyril W Hirt and Billy D Nichols. “Volume of fluid (VOF) method for the dynamics of free boundaries”. In: *Journal of computational physics* 39.1 (1981), pp. 201–225.

[137] Mark Sussman et al. “An improved level set method for incompressible two-phase flows”. In: *Computers & Fluids* 27.5-6 (1998), pp. 663–680.

[138] Thomas Leyssens et al. “A Delaunay refinement algorithm for the particle finite element method applied to free surface flows”. In: *International Journal for Numerical Methods in Engineering* (2024), e7554.

[139] Joe J Monaghan. “Smoothed particle hydrodynamics”. In: *Reports on progress in physics* 68.8 (2005), p. 1703.

[140] Deborah Sulsky, Zhen Chen, and Howard L Schreyer. “A particle method for history-dependent materials”. In: *Computer methods in applied mechanics and engineering* 118.1-2 (1994), pp. 179–196.

[141] Andrea Pasqua, Alessandro Leonardi, and Marina Pirulli. “Coupling Depth-Averaged and 3D numerical models for the simulation of granular flows”. In: *Computers and Geotechnics* 149 (2022), p. 104879.

[142] Célestin Marot, Jeanne Pellerin, and Jean-François Remacle. “One machine, one minute, three billion tetrahedra”. In: *International Journal for Numerical Methods in Engineering* 117.9 (2019), pp. 967–990.

[143] Jia Mao et al. “A resolved CFD–DEM approach for the simulation of landslides and impulse waves”. In: *Computer Methods in Applied Mechanics and Engineering* 359 (2020), p. 112750.

[144] Fengze Xie, Weiwen Zhao, and Decheng Wan. “Numerical simulations of liquid-solid flows with free surface by coupling IMPS and DEM”. In: *Applied Ocean Research* 114 (2021), p. 102771.

[145] Xiaosong Sun, Mikio Sakai, and Yoshinori Yamada. “Three-dimensional simulation of a solid–liquid flow by the DEM–SPH method”. In: *Journal of Computational Physics* 248 (2013), pp. 147–176.

[146] Alessandro Franci et al. “3D simulation of Vajont disaster. Part 1: Numerical formulation and validation”. In: *Engineering Geology* 279 (2020), p. 105854.

[147] Herbert Edelsbrunner, David Kirkpatrick, and Raimund Seidel. “On the shape of a set of points in the plane”. In: *IEEE Transactions on information theory* 29.4 (1983), pp. 551–559.

[148] L Paul Chew. “Guaranteed-quality mesh generation for curved surfaces”. In: *Proceedings of the ninth annual symposium on Computational geometry* (1993), pp. 274–280.

[149] Pratik Suchde and Jörg Kuhnert. “Point cloud movement for fully Lagrangian meshfree methods”. In: *Journal of Computational and Applied Mathematics* 340 (2018), pp. 89–100.

[150] Marco Lucio Cerquaglia et al. “Free-slip boundary conditions for simulating free-surface incompressible flows through the particle finite element method”. In: *International Journal for numerical methods in engineering* 110.10 (2017), pp. 921–946.

[151] Eugenio Onate et al. “Advances in the particle finite element method (PFEM) for solving coupled problems in engineering”. In: *Particle-based methods: fundamentals and applications* (2011), pp. 1–49.

[152] Manon Robbe-Saule et al. “Experimental investigation of tsunami waves generated by granular collapse into water”. In: *Journal of Fluid Mechanics* 907 (2021), A11.

[153] Severin Strobl, Arno Formella, and Thorsten Pöschel. “Exact Calculation of the Overlap Volume of Spheres and Mesh Elements”. In: *Journal of Computational Physics* 311 (Apr. 2016), pp. 158–172. ISSN: 0021-9991. DOI: 10.1016/j.jcp.2016.02.003.

[154] Ellis Horowitz and Marco Papa. “Polygon clipping: Analysis and experiences”. In: *Theoretical Studies in Computer Science*. Elsevier, 1992, pp. 315–339.

[155] Inbar Vaknin et al. “Gas seepage and pockmark formation from subsurface reservoirs: Insights from table-top experiments”. In: *Journal of Geophysical Research: Solid Earth* 129.4 (2024), e2023JB028255.

[156] Erik Burman and Paolo Zunino. “Numerical approximation of large contrast problems with the unfitted Nitsche method”. In: *Frontiers in Numerical Analysis-Durham 2010*. Springer, 2011, pp. 227–282.

[157] Peter Hansbo and Mats G Larson. “Nitsche’s finite element method for model coupling in elasticity”. In: *Computer Methods in Applied Mechanics and Engineering* 392 (2022), p. 114707.